Inverse delta doping for improvement of solar cells

K. W. Böer and J. Piprek
Material Science Program, College of Engineering, University of Delaware, Newark, Delaware 19716

(Received 19 July 1993; accepted for publication 8 February 1994)

Delta doping with deep-level centers results in a marked decrease of open-circuit voltage and fill factor of photodiodes and solar cells when the doped layer is located near the crossover of electron and hole densities. The omission of recombination centers in a thin layer (inverse delta doping) at this position consequently causes an increase of the open-circuit voltage. The difficulty of improving the open-circuit voltage in actual high-efficient solar cells may have its origin in the inadvertent creation of donor-acceptor pairs caused by cross doping and consequent compensation. Such pairs are known to act as efficient recombination centers. The insertion of a thin, undoped interlayer is proposed to separate donors and acceptors and thereby reduce the density of close pairs.

I. INTRODUCTION

Junction recombination is known to degrade the diode performance.[1] Such recombination is the major contributor to a reduction of open circuit voltage V_{oc} and fill factor (FF) in solar cells, as it increases the junction leakage, i.e., the reverse saturation current. In this article we investigate in more detail the losses near the junction interface of photodiodes (at low optical generation rates) and of solar cells (with sunlight excitation). For this, the solution curves of transport, continuity, and Poisson equations of a two-carrier model are analyzed, using a GaAs p-n junction as an example.

Earlier investigations[2-4] have shown that the degradation of the performance of solar cells by recombination centers is sensitive to the position of their incorporation relative to the junction interface. In order to examine this, we have proposed delta doping with such centers, i.e., by inserting a thin layer with increased density of deep-level centers at various positions parallel to the metallurgical junction interface. Starting with a short summary of this delta-doped case,[4] we then focus our investigation on such devices containing a thin layer that has a decreased density of recombination centers (inverse-delta-doped layer). For an inverse delta doping in actual solar cells we assume a reduction of donor-acceptor pairs that usually enhance recombination. Thus, we finally also analyze a reduction of donors and acceptors within the inverse-delta-doped layer.

II. GOVERNING SET OF EQUATIONS AND PARAMETERS

The well-known set of governing equations for an essentially one-dimensional x device consists of the transport equations

$$j_n = e\mu_n n \frac{dV}{dx} + \mu_n kT \frac{dn}{dx}, \tag{1}$$

$$j_p = e\mu_p p \frac{dV}{dx} - \mu_p kT \frac{dp}{dx}, \tag{2}$$

the stationary continuity equations

$$\frac{dj_n}{dx} = e(R-G), \tag{3}$$

$$\frac{dj_p}{dx} = e(G-R), \tag{4}$$

and the Poisson equation [Eq. (8), below]. The generation-recombination (GR) current is composed of the thermal and optical generation and the compensating recombination. The recombination rate is obtained from the Shockley–Read–Hall model[5]

$$R = \frac{np}{\tau_p(n+n_i^+) + \tau_n(p+n_i^-)}, \quad n_i^{\pm} = n_i \exp\left(\pm\frac{E_r - E_i}{kT}\right), \tag{5}$$

with the intrinsic density $n_i = 2.1\times10^6$ cm^{-3} and the intrinsic level $E_i = E_c - 0.67$ eV for GaAs at room temperature. The direct energy gap of GaAs is $E_g = E_c - E_v = 1.424$ eV. The effective densities of states in both bands are $N_c = 4.21\times10^{17}$ cm^{-3} and $N_v = 9.51\times10^{18}$ cm^{-3}. E_r is the energy of the recombination center. Here, we are analyzing recombination centers at a discrete energy level $E_r = E_i$, hence their influence is expected to depend on the local position of the centers within the junction. The carrier lifetimes are given by

$$\tau_{n,p} = (v_{\mathrm{rms}(n,p)} s_{n,p} N_r)^{-1}, \tag{6}$$

with $s_{n,p}$ denoting the capture cross sections for electrons and holes and N_r describing the density of recombination centers.

The generation rate contains a thermal and an optical part,

$$G = \frac{n_i^2}{\tau_p(n+n_i^+) + \tau_n(p+n_i^-)} + g_o. \tag{7}$$

For reasons of ease of interpretation, the optical excitation rate g_o is first assumed to be homogeneous. To compare with a practical sample $g_o(x)$ is then calculated for air mass (AM) 1.5 illumination.

 0021-8979/94/75(10)/5095/7/$6.00 © 1994 American Institute of Physics

Downloaded 22 Nov 2005 to 128.175.13.10. Redistribution subject to AIP license or copyright, see http://jap.aip.org/jap/copyright.jsp

TABLE I. Parameters used for computation of solution curves for the thin, symmetrically doped GaAs cell.

Name	Symbol	Value	Unit
Thickness of the n region	d_n	0.2	μm
Thickness of the p region	d_p	0.2	μm
Donor density (n region)	N_d	10^{17}	cm^{-3}
Acceptor density (p region)	N_a	10^{17}	cm^{-3}
Bulk electron lifetime (both regions)	τ_n	10^{-7}	s
Bulk hole lifetime (both regions)	τ_p	10^{-7}	s
Bulk electron mobility	$\mu_{n,0}$	3000	$cm^2/(V\,s)$
Bulk hole mobility	$\mu_{p,0}$	265	$cm^2/(V\,s)$
Surface recombination velocity, front	S_F	0	cm/s
Surface recombination velocity, back	S_B	0	cm/s

The Poisson equation takes into account both carriers, as well as charged shallow and deep-level defects,

$$\epsilon\epsilon_0 \frac{d^2V}{dx^2} = e(n-p+N_a-N_d+n_r), \tag{8}$$

with the shallow donors and acceptors assumed to be fully ionized, and the density of charged deep-level centers n_r determined by the Shockley–Read–Hall occupation rate

$$f_r = \frac{\tau_n n + \tau_p n_i^-}{\tau_n(n+n_i^+) + \tau_p(p+n_i^-)}. \tag{9}$$

The electron and hole mobilities are considered as field dependent[6] following the gradients F_n and F_p of the corresponding quasi-Fermi level. Because of electron scattering into the side valleys of the conduction band, the electron mobility is[7]

$$\mu_n = \frac{\mu_{n,0} + v_n^*(F_n^3/F_c^4)}{1+(F_n/F_c)^4}, \tag{10}$$

with $v_n^* = 8.5 \times 10^6$ cm/s and F_c=4 kV/cm giving the electron saturation drift velocity and the critical field for electron redistribution in GaAs, respectively.

The solution curves of this set are computed using finite element analysis of the PC-1D software package,[8] modified by charged deep levels and the proper electrochemical-field dependence of the mobility.[9] The used parameters of the analyzed GaAs devices are listed in Tables I and II, respectively. Parameters that are specific for certain sets of solution curves are given in the respective figure captions.

For the investigation of delta doping and inverse delta doping of deep-level recombination centers in solar cells we start with a thin, symmetrical GaAs p-n junction photodiode (see Table I) exposed to a relatively low and homogeneous optical recombination rate of $g_o = 10^{16}$ cm^{-3}/s.

As boundary condition to both outer surfaces we have used neutral electrode conditions, i.e., a horizontal connection of the majority quasi-Fermi level to the electrode without a collapse of the minority quasi-Fermi level. Thereby we neglect the influence of additional space-charge regions in front of, and carrier recombination at, both electrodes. *In praxi* this can be approximated by interfacing the active part of the device and the electrodes with a highly doped n^+ or p^+ layer.

TABLE II. Parameters from a MOVPE-grown GaAs solar cell with asymmetrical doping (see Ref. 10). This example is chosen since all relevant parameters are given, even though it is not one of the highest efficient cells, probably because of insufficient surface passivation (such passivation via an $Al_{0.8}Ga_{0.2}As$ window typically reduces the surface recombination velocity to values below 10^5 cm/s at the front, and at the back the surface recombination velocity at the base/back-surface-field interface lies typically below 10^4 cm/s, yielding conversion efficiencies above 23%).

Name	Symbol	Value	Unit
Thickness of the n region (base)	d_n	4.0	μm
Thickness of the p region (emitter)	d_p	0.6	μm
Donor density (n region)	N_d	3×10^{17}	cm^{-3}
Acceptor density (p region)	N_a	1×10^{18}	cm^{-3}
Bulk electron lifetime (both regions)	τ_n	5×10^{-10}	s
Bulk hole lifetime (both regions)	τ_p	5×10^{-9}	s
Bulk electron mobility	$\mu_{n,0}$	3000	$cm^2/(V\,s)$
Bulk hole mobility	$\mu_{p,0}$	150	$cm^2/(V\,s)$
Surface recombination velocity, front	S_F	10^6	cm/s
Surface recombination velocity, back	S_B	10^6	cm/s

III. INFLUENCE OF DELTA DOPING

Into this simplified GaAs photodiode, a thin sheet with additional doping of deep-level centers is introduced, resulting in a reduced carrier lifetime. Since the boundaries of this sheet are abrupt, and its width is typically only a few atomic layers, we refer to it as a delta-doped sheet. The change in charge densities between the sheet and its surrounding is small enough to neglect complications of the level spectrum by quantum-well effects.[6] Figure 1 shows the changes in the current density-voltage (j-V) characteristics when inserting a

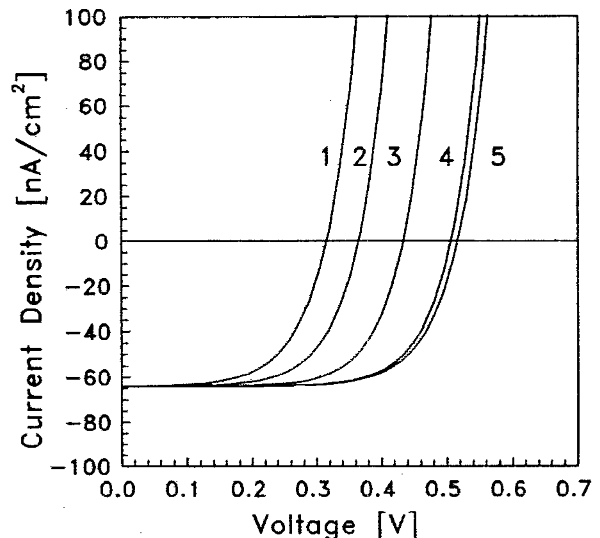

FIG. 1. j-V characteristics of thin symmetrically doped GaAs photodiodes with homogeneous optical generation rates of $g_o = 10^{16}$ cm^{-3} s^{-1} with delta-doped deep levels within a layer of 5 nm thickness, resulting in a minority-carrier lifetime within this layer of $\tau = 10^{-9}$ s. The delta-doped sheet is placed at the p side with the distance from the metallurgical interface of 0, 5, 10, and 20 nm for curves 1–4 respectively. Curve 5 is computed without delta-doped layer. The carrier lifetime in both sides of the device is assumed as 10^{-7} s.

Downloaded 22 Nov 2005 to 128.175.13.10. Redistribution subject to AIP license or copyright, see http://jap.aip.org/jap/copyright.jsp

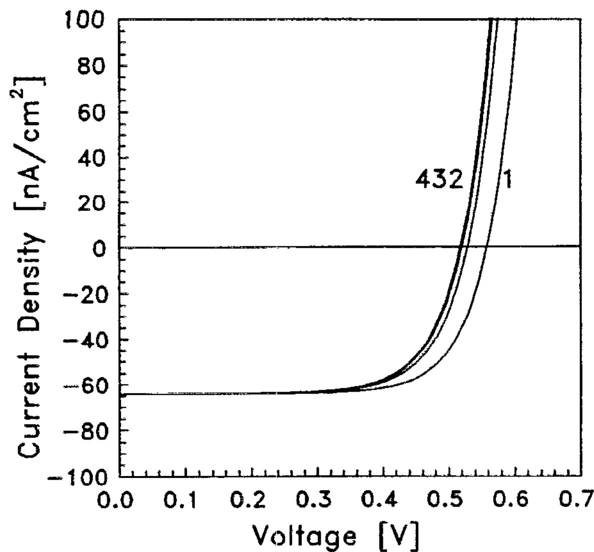

FIG. 2. j-V characteristics as in Fig. 1, however, with an inverse-delta-doped layer of 5 nm thickness and a reduced density of deep-level centers, resulting in a minority-carrier lifetime of $\tau=10^{-5}$ s. The shift of the center plane of this sheet from the metallurgical boundary of the p-n junction is 0, 5, and 10 nm for curves 1–3, respectively. Curve 4 is computed without an interlayer and it is almost identical to curve 3.

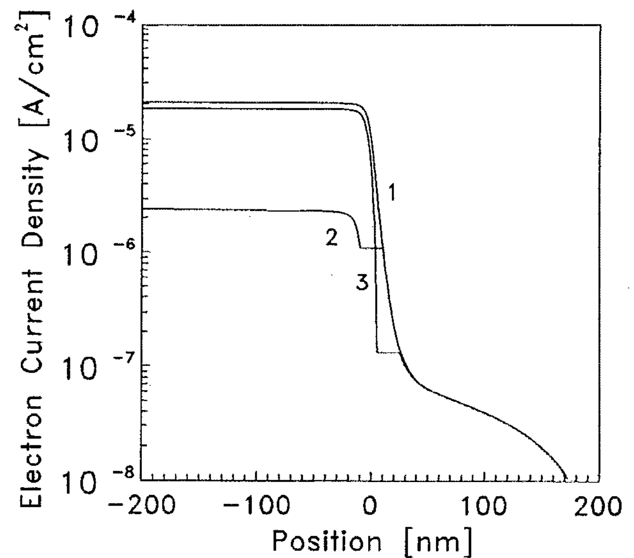

FIG. 3. Electron current distribution $j_n(x)$ in the photodiode given in Fig. 2: (1) with no interlayer; (2) for an inverse-delta-doped sheet of 20 nm thickness at the metallurgical interface ($x=0$); and (3) with that sheet shifted by 15 nm into the p-type region. The minority-carrier lifetime in the inverse-delta-doped sheet is 10^{-5} s.

delta-doped layer with deep-level defect centers thereby reducing the minority-carrier lifetime from 10^{-7} s in the rest of the device to 10^{-9} s within this layer. The family parameter is the distance of the center plane of this layer from the metallurgical interface. From Fig. 1 it is evident that substantial performance degradation takes place only when the delta-doped layer is close to the interface.

The increase in the junction recombination current is an increase in the dark GR current, hence an increase in the reverse dark saturation current density j_0 leading to a logarithmic decrease in the open-circuit voltage, as obtained from the basic diode characteristic,

$$j=j_0\left[\exp\left(\frac{eV}{AkT}\right)-1\right]-j_L, \quad (11)$$

yielding for $j=0$

$$V_{oc}=\frac{AkT}{e}\ln\left(\frac{j_L}{j_0}\right), \quad (12)$$

i.e., one would expect for a change of τ by a factor of 100 a shift of approximately 120 mV, assuming a diode quality factor $A=1$. The computed shift of the open-circuit voltage is about a factor of 2 larger, indicating that the characteristic is in a range where $A\simeq2$ when the delta-doped layer is inserted close to the metallurgical interface of this example device.

IV. INVERSE DELTA DOPING

From the results given above, it is suggestive to insert a layer in which the density of recombination centers is reduced. We will call such a layer an inverse-delta-doped layer.

Figure 2 shows the result for the same device as shown in Fig. 1 except with an inserted thin layer that has a density of recombination centers that is reduced by a factor of 0.01 compared to the rest of the device. This results in an increase of the open-circuit voltage when the sheet approaches the interface.

The position sensitivity of the inverse-delta-doped sheet can be understood by plotting the generation-recombination current within the junction region without optical excitation. This is shown for the electron GR current $j_n(x)$ in Fig. 3. The maximum slope occurs at the position where $n\simeq p$ for a normal p-n junction (curve 1). When an inverse-delta-doped layer with a lower recombination rate is introduced, the slope of j_n (and of j_p, not shown here) is reduced within this layer (here by a factor of 0.01). When the layer is positioned where the slope of a normal device was the largest, the reduction of the accumulated GR current is largest, as seen in curve 2. When the inverse-delta-doped layer is moved away from this optimal position, its beneficial effect is substantially reduced (curve 3).

The open-circuit voltage and the fill factor of a properly positioned sheet increase with increasing sheet width δ as shown in Fig. 4. However, the effectiveness of such improvement rapidly decreases with increasing layer thickness, as regions of lesser original recombination are being replaced by the inverse-delta-doped sheet.

The position sensitivities of an inserted delta-doped or inverse-delta-doped sheet of 5 nm width with a factor 0.01 or 100 changed lifetime compared to the rest of the device are shown in Fig. 5. It becomes obvious that the effect of inverse delta doping is even more position sensitive than for delta doping, and that only well-placed inverse-delta-doped sheets have a beneficial effect on the device performance.

For the full benefit of the V_{oc} improvement, it suffices to have the recombination center density reduced by two orders

Downloaded 22 Nov 2005 to 128.175.13.10. Redistribution subject to AIP license or copyright, see http://jap.aip.org/jap/copyright.jsp

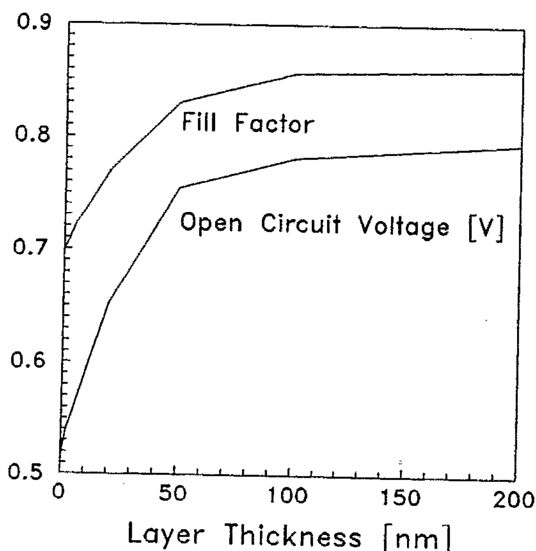

FIG. 4. The improvement of V_{oc} and FF as a function of the inverse-delta-doped layer thickness δ for the symmetrical p-n junction diode as given in Table I. The inserted layer remains centered at the metallurgical boundary and has a minority-carrier lifetime of $\tau = 10^{-5}$ s.

of magnitude, with most of the shift already achieved when N_r is reduced by a factor of 0.1 (see Fig. 6).

The photogeneration rate dependency of the effect of an incorporated delta-doped or inverse-delta-doped sheet can best be judged from the forward-biased dark j-V characteristics, shown in Fig. 7 for the symmetrically doped device that contains an inserted layer of 5 nm thickness, centered at the metallurgical interface. The lifetime in this layer is given as the family parameter. When considering the superposition principle, the open-circuit voltage can be directly read from the intersection of these curves with a horizontal line at the photocurrent level (=the short-circuit current).

From the family of curves shown in Fig. 7 it is evident that the insertion of a delta layer with different minority-carrier lifetime has a larger effect on V_{oc} at low optical excitation rates than at rates that are typical for sunlight and yielding short-circuit current densities in the 20–40 mA/cm^2 range. Here, the curves approach closer the case without a delta layer (i.e., the dashed curve in Fig. 7). Inverse delta doping shows little effect at these light intensities. Therefore, one would expect that actual high-efficient solar cells show V_{oc} and FF values that approach closely their theoretical limits, obtained from minority-carrier lifetime values measured in the device; however, this is not the case.

V. INVERSE DELTA DOPING IN ASYMMETRICAL SOLAR CELLS

In variance to the simplified symmetrical diode example, actual solar cells are usually asymmetrically doped and the optical generation rate g_o decreases with the penetration depth of the light according to the spectrum.

For comparison with the computation of such a cell we have used parameters from an actual GaAs solar cell[10] grown by metal-organic vapor-phase epitaxy (MOVPE) with a

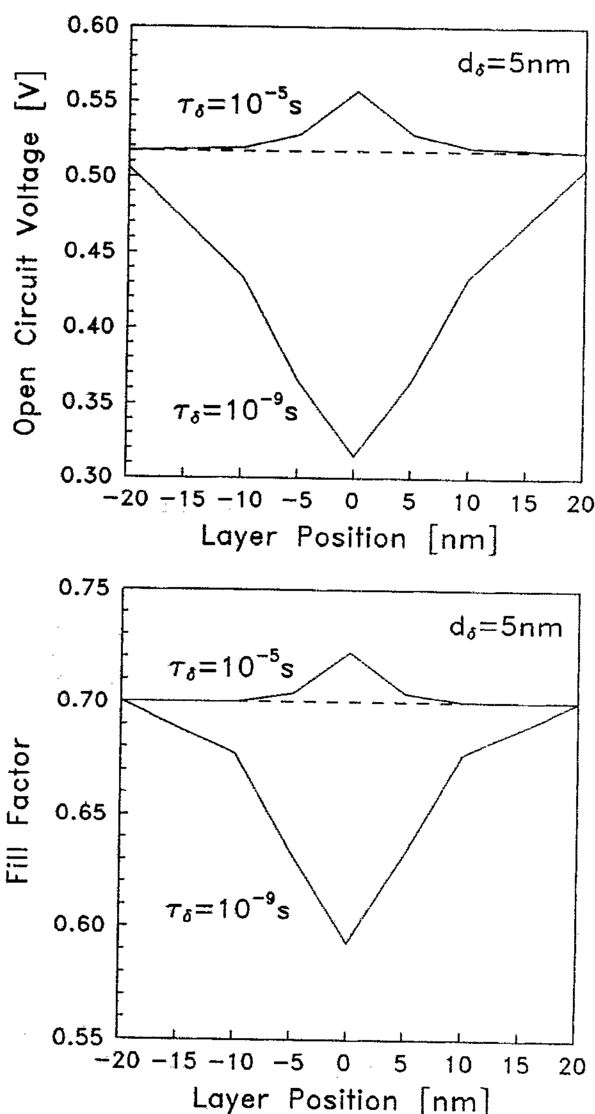

FIG. 5. V_{oc} and FF of the same devices as given in the previous figures as a function of the position of the center of the inserted sheet of 5 nm thickness and 10^{-9} or 10^{-5} s minority-carrier lifetime for the delta-doped (lower curves) or inverse-delta-doped (upper curves) layers, respectively.

p-type emitter and an abrupt p-n junction (see Table II). Here, we recalculated the bulk electron and hole lifetime according to a diffusion length of about 2 μm (a critical parameter in the computation that in Ref. 10 is roughly estimated as 10^{-10} and 10^{-9} s, respectively).

The measured solar-cell performance data reported in Ref. 10 under AM 1.5 illumination are listed in Table III. The photocurrent density of 23 mA/cm^2 corresponds to a light intensity of 100 mW/cm^2. The spatial distribution of the optical generation rate $g_o(x)$ is given by the internal PC-1D computation. With the values in Table II the calculated V_{oc} value lies about 20 mV above the measured one, and fill factor and efficiency are also higher than *in praxi* (see Table III, $\tau_\delta/\tau_{bulk}=1$). This is taken as an indication that additional recombination centers are present near the critical position close to the junction interface that reduce the carrier lifetime

Downloaded 22 Nov 2005 to 128.175.13.10. Redistribution subject to AIP license or copyright, see http://jap.aip.org/jap/copyright.jsp

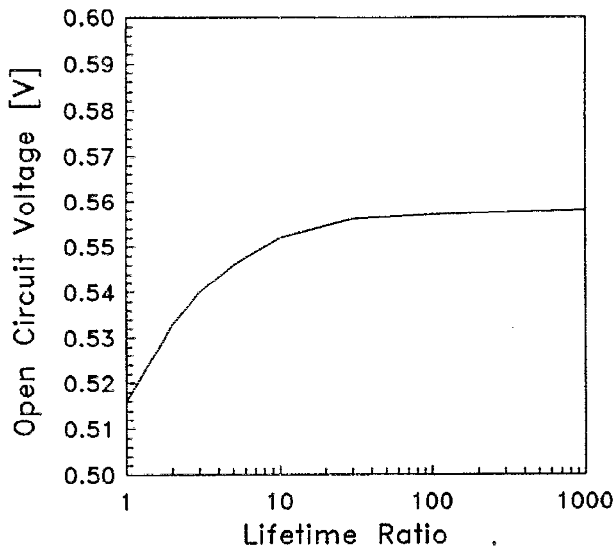

FIG. 6. V_{oc} improvement as a function of the ratio of lifetimes within the inverse-delta-doped layer to that of the remainder of the symmetrical device of Table I. A layer width of 5 nm is assumed.

below the value measured in the bulk and listed in Table II (see Sec. VI).

Most recombination centers are asymmetric, i.e., their capture coefficient for electrons is different from the corresponding coefficient for holes; moreover, the effective masses of electrons and holes are different. This results in a different lifetime for electrons and holes. Therefore, the position of maximum recombination via a deep level is not exactly at the p-n intersection.

TABLE III. Performance parameters of an actual GaAs solar cell as measured (see Ref. 10) and as computed with a delta-doped sheet of 15 nm width next to the p-n interface at the n side (varying the lifetime ratio between interlayer and bulk) and a uniform photocurrent density of 23 mA/cm^2.

			V_{oc} (V)	FF	η (%)
Measurement			0.934	0.786	16.9
Calculation	τ_δ/τ_{bulk}	=0.33	0.934	0.811	17.4
		=1	0.955	0.836	18.4
		=10	0.964	0.867	19.2
		=100	0.965	0.871	19.3
		=1000	0.965	0.871	19.3

This position of highest sensitivity is shifted from the metallurgical interface into the lower-doped region by a distance on the order of the Debye length[11]—in our case it is shifted by about 10 nm (depending on the bias) into the lower-doped n region. Therefore, a 15-nm-thick interlayer that sufficiently covers the recombination sensitive region is introduced at the n side, attached to the p-n interface. Figure 8 shows the computed dark j-V characteristics for the interlayer lifetimes given in Table III. Compared with the dark j-V characteristics of the symmetrical diode (Fig. 7), the inverse delta doping has more influence on the asymmetrical solar cell, at higher optical generation, even with sunlight photocurrent (dotted line in Fig. 8).

The measured open-circuit voltage can be reproduced by the simulation when the lifetime in this layer is reduced to one-third of the bulk value (see Table III for τ_δ/τ_{bulk}=0.33), i.e., the investigated sample seems to have a three times higher recombination center density near the junction than in

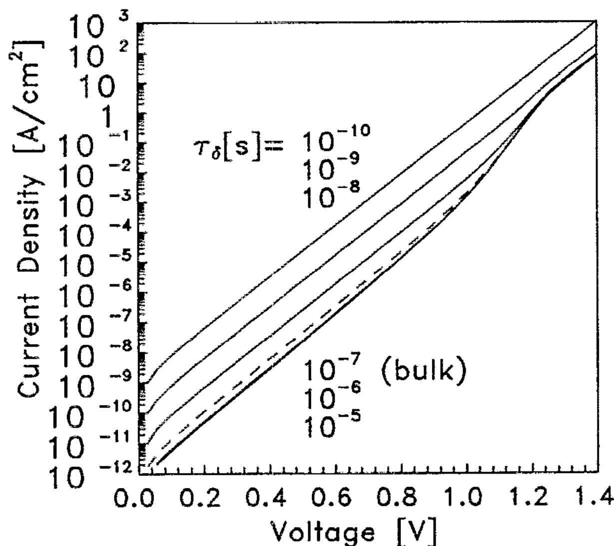

FIG. 7. Dark j-V characteristics in forward bias of the symmetrically doped device as in previous figures and with an inserted layer of 5 nm thickness, centered at the metallurgical interface. The lifetime of minority carriers within this layer is given as the family parameter. The dashed curve is computed without interlayer (τ_δ=10^{-7} s), the curves with τ_δ=10^{-6} s and τ_δ=10^{-5} s are almost identical.

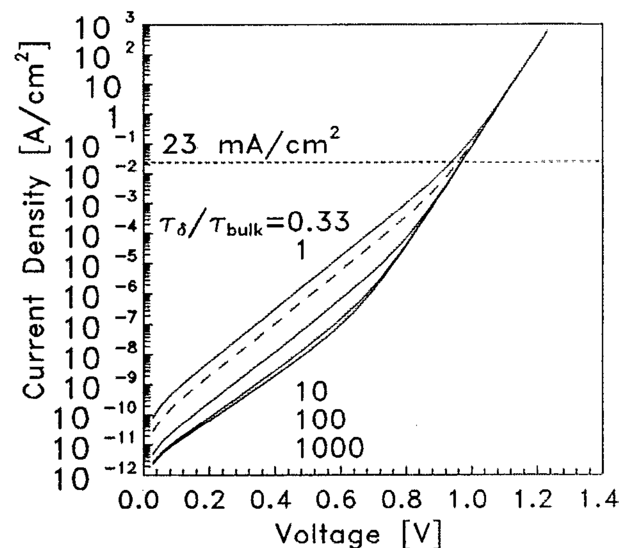

FIG. 8. Computed dark j-V characteristics in forward bias of the asymmetrical solar cell according to Table II with an inserted layer of 15 nm thickness at the n side, attached to the metallurgical interface. The lifetime ratio of minority carriers between this layer and the bulk is given as the family parameter. The measured photocurrent density of 23 mA/cm^2 is indicated as dotted line.

Downloaded 22 Nov 2005 to 128.175.13.10. Redistribution subject to AIP license or copyright, see http://jap.aip.org/jap/copyright.jsp

the bulk (see discussion in Sec. VI). The computed fill factor, hence the efficiency, is still higher than in the real device, probably due to additional loss mechanisms.

Avoiding additional recombination centers near the p-n junction improves V_{oc} by 20 mV. Introducing an inverse-delta-doped sheet further improves V_{oc} by another 10 mV, as shown in Table III for rising lifetime ratio τ_δ/τ_{bulk}. Taking both measures together, the fill factor can gain a value of 0.06 and the efficiency is increased by about two percentage points.

VI. DONOR-ACCEPTOR PAIRS AS UNINTENTIONAL RECOMBINATION CENTERS

For actual GaAs devices only the short-circuit current can be brought close to the theoretical limit, while open-circuit voltage and fill factor lie substantially below their theoretical limit that is computed with experimentally determined cell parameters, including the minority-carrier lifetimes in the n and p region of the device. This indicates that additional recombination centers always remain close to the intersection of $n(x)$ and $p(x)$ which are not easily detected by conventional means. Donor-acceptor pairs[6] could act as such recombination centers at the junction interface even in ultraclean (except for shallow donors or acceptors) semiconductors. Such pairs are plentiful at and near the metallurgical interface.

It is therefore suggestive to also reduce the density of shallow dopants in the inverse-delta-doped layer. When doing this without lowering the density of recombination centers, a decrease of the open-circuit voltage is computed which is largest when the center plane coincides with the p-n intersection and increases with the thickness of this interlayer.

However, such a reduction of the shallow dopant density does not change the improvement by inverse delta doping as discussed in the previous section as long as this layer is less than 10 nm thick (see Fig. 9). If such a thin layer indeed reduces substantially the density of close donor-acceptor pairs, and thereby by itself the recombination traffic, it produces the same benefit as a layer of similar width that has a reduced density of conventional recombination centers (e.g., of deep-level centers).

With larger width of this layer, the resulting V_{oc} and FF improvements in Fig. 9 are somewhat smaller with decreasing density of shallow dopants. This is probably caused by a reduced effectiveness of the p-n junction due to a more severe perturbation of its space-charge distribution. The figure also shows that a shallow doping reduction by one order of magnitude already yields near saturation of the depicted effect.

It is, however, a different question to judge to what extent such an interlayer reduces the recombination via donor-acceptor pairs. This problem cannot be answered within the frame of this article. We may only speculate at this point that close pairs that are Coulomb bound to each other may accumulate during conventional processing, while distant pairs remain statistically distributed and therefore at lower concentration. This could explain a lower recombination even though distant pairs have a similar recombination cross section because of the substantial remaining overlap of their hydrogenlike eigenfunctions.

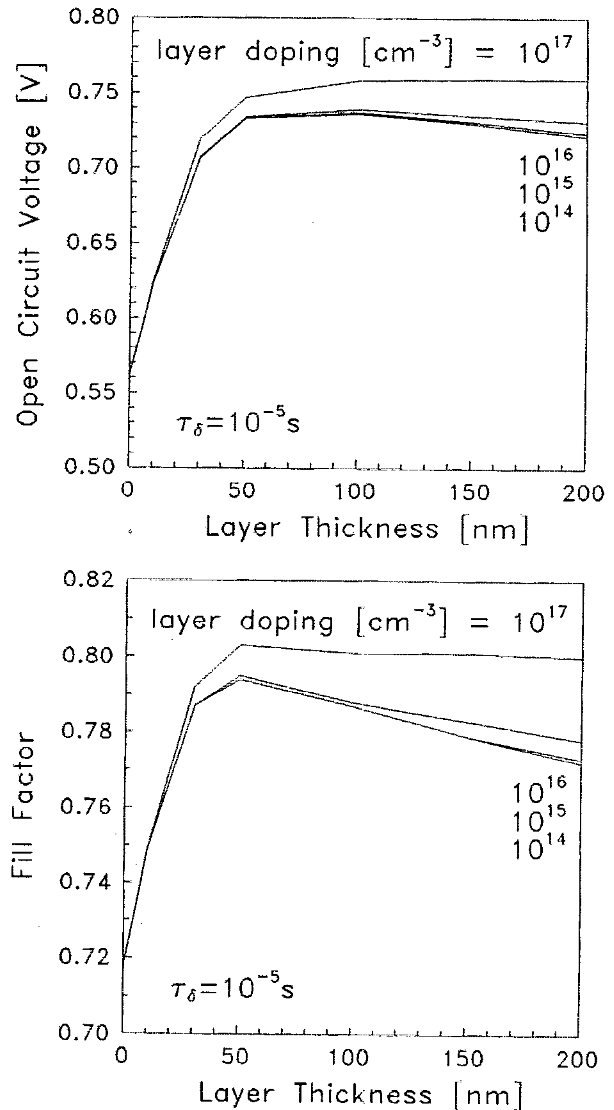

FIG. 9. V_{oc} and FF as a function of the thickness of a layer that contains a lowered density of shallow donors and acceptors (a pseudo-i layer) and is centered at the metallurgical boundary of a symmetrical p-n junction as given in Table I. The donor and (equal) acceptor densities in this inverse-delta-doped layer are given as family parameters. The minority-carrier lifetime in the pseudo-i layer is increased to 10^{-5} s (compared to 10^{-7} s in the remainder). For comparison, the upper curves show the case with maintained shallow doping. The total device thickness is increased to 1 μm in order to keep the inverse-delta-doped region only at a small fraction of the device.

This therefore suggests to insert (e.g., by molecular-beam epitaxy) an approximately 10 nm thin inverse-delta-doped layer that has a somewhat lowered density of shallow and of deep-level dopants. A lowering by one to two orders

Downloaded 22 Nov 2005 to 128.175.13.10. Redistribution subject to AIP license or copyright, see http://jap.aip.org/jap/copyright.jsp

of magnitude seems to be sufficient for a substantial performance improvement, as long as this layer is positioned appropriately.

VII. SUMMARY

We have shown that the insertion of a thin layer with a high density of recombination centers degrades the performance of a solar cell substantially only when it is introduced near the crossover of electron and hole densities. That means that the insertion of a similar amount of recombination centers at other positions within the solar cell is totally benign, i.e., does not degrade the performance of the cell.

Inversely, the introduction of a thin layer with a reduced density of recombination centers at this position causes an improvement of open-circuit voltage and fill factor. The improvement saturates with a decrease of recombination by one to two orders of magnitude, and with a layer thickness of about 50 nm. The position sensitivity of the cell improvement is rather steep (±5 nm for the presented example of a GaAs *p-n* junction). In actual solar cells, such an inverse-delta-doped layer should include the reduction of close donor-acceptor pairs which otherwise act as *unintentionally* introduced recombination centers.

[1] C. T. Sah, R. N. Noyce, and W. Shockley, Proc. IRE **45**, 859 (1955).
[2] A. Y. Ali and K. W. Böer, in Proceedings of the 18th IEEE Photovoltaic Specialists Conference, Las Vegas, 1985, p. 1739.
[3] A. Y. Ali and K. W. Böer, Sol. Cells **21**, 263 (1986).
[4] J. Piprek, H. Kostial, P. Krispin, C. H. Lange, and K. W. Böer, Proc. SPIE **1679**, 232 (1992).
[5] W. Shockley and W. T. Read, Jr., Phys. Rev. **87**, 835 (1952); R. N. Hall, *ibid.* **87**, 387 (1952).
[6] K. W. Böer, *Survey of Semiconductor Physics* (Van Nostrand Reinhold, New York, 1990), Vol. 1, Chap. 33.
[7] S. Selberherr, *Analysis and Simulation of Semiconductor Devices*, (Springer, Vienna, 1984), p. 97.
[8] P. Basore, IEEE Trans. Electron Devices **ED-37**, 337 (1990).
[9] J. Piprek, P. Krispin, H. Kostial, C. H. Lange, and K. W. Böer, Phys. Status Solidi B **173**, 661 (1992).
[10] W. G. J. H. M. van Sark, B. F. P. Jansen, X. Tang, L. J. Giling, and W. Crans, Sol. Cells **29**, 319 (1990).
[11] K. W. Böer, *Survey of Semiconductor Physics* (Van Nostrand Reinhold, New York, 1992), Vol. 2, Chap. 23.

Downloaded 22 Nov 2005 to 128.175.13.10. Redistribution subject to AIP license or copyright, see http://jap.aip.org/jap/copyright.jsp